4774–4790 *Nucleic Acids Research, 2023, Vol. 51, No. 10* *Published online 17 March 2023*
https://doi.org/10.1093/nar/gkad167

The novel GATA1-interacting protein HES6 is an essential transcriptional cofactor for human erythropoiesis

Zi Wang[1,*,†], Pan Wang[1,†], Jieying Zhang[1,2], Han Gong[1], Xuchao Zhang[1], Jianhui Song[3], Ling Nie[3], Yuanliang Peng[1], Yanan Li[1], Hongling Peng[1], Yajuan Cui[1], Heng Li[1], Bin Hu[1], Jun Mi[2], Long Liang[1], Hong Liu[3], Ji Zhang[4], Mao Ye[5], Karina Yazdanbakhsh[6], Narla Mohandas[7], Xiuli An[8], Xu Han[1,*] and Jing Liu[1,*]

[1]Department of Hematology, The Second Xiangya Hospital of Central South University; Molecular Biology Research Center, Center for Medical Genetics, School of Life Sciences; Hunan Province Key Laboratory of Basic and Applied Hematology, Central South University, Changsha 410011, China, [2]Basic Medical Institute; Hongqiao International Institute of Medicine, Tongren Hospital; Key Laboratory of Cell Differentiation and Apoptosis of Chinese Ministry of Education, Shanghai Jiao Tong University School of Medicine, Shanghai 200025, China, [3]Xiangya Hospital, Central South University, Changsha 410008, China, [4]Department of Clinical Laboratory, the First Affiliated Hospital, University of South China, Hengyang 421001, China, [5]Molecular Science and Biomedicine Laboratory, State Key Laboratory for Chemo/Biosensing and Chemometrics; College of Biology; College of Chemistry and Chemical Engineering, Hunan University, Changsha 410082, China, [6]Laboratory of Complement Biology, NY Blood Center, NY 10065, USA, [7]Red Cell Physiology Laboratory, NY Blood Center, NY 10065, USA and [8]Laboratory of Membrane Biology, NY Blood Center, NY 10065, USA

Received October 08, 2022; Revised February 21, 2023; Editorial Decision February 21, 2023; Accepted March 15, 2023

ABSTRACT

Normal erythropoiesis requires the precise regulation of gene expression patterns, and transcription cofactors play a vital role in this process. Deregulation of cofactors has emerged as a key mechanism contributing to erythroid disorders. Through gene expression profiling, we found HES6 as an abundant cofactor expressed at gene level during human erythropoiesis. HES6 physically interacted with GATA1 and influenced the interaction of GATA1 with FOG1. Knockdown of HES6 impaired human erythropoiesis by decreasing GATA1 expression. Chromatin immunoprecipitation and RNA sequencing revealed a rich set of HES6- and GATA1-co-regulated genes involved in erythroid-related pathways. We also discovered a positive feedback loop composed of HES6, GATA1 and STAT1 in the regulation of erythropoiesis. Notably, erythropoietin (EPO) stimulation led to upregulation of these loop components. Increased expression levels of loop components were observed in CD34^{+} cells of polycythemia vera patients. Interference by either HES6 knockdown or inhibition of STAT1 activity suppressed proliferation of erythroid cells with the JAK2^{V617F} mutation. We further explored the impact of HES6 on polycythemia vera phenotypes in mice. The identification of the HES6–GATA1 regulatory loop and its regulation by EPO provides novel insights into human erythropoiesis regulated by EPO/EPOR and a potential therapeutic target for the management of polycythemia vera.

*To whom correspondence should be addressed. Tel: +86 731 84805026; Fax: +86 731 84805026; Email: jingliucsu@hotmail.com; liujing2018@csu.edu.cn
Correspondence may also be addressed to Xu Han. Tel: +86 731 84805449; Fax: +86 731 84805449; Email: hx1989345@163.com
Correspondence may also be addressed to Zi Wang. Tel: +86 731 84805449; Fax: +86 731 84805449; Email: 220144@csu.edu.cn; zhongnanwangzi@126.com
†The authors wish it to be known that, in their opinion, the first two authors should be regarded as Joint First Authors.

© The Author(s) 2023. Published by Oxford University Press on behalf of Nucleic Acids Research.
This is an Open Access article distributed under the terms of the Creative Commons Attribution-NonCommercial License (http://creativecommons.org/licenses/by-nc/4.0/), which permits non-commercial re-use, distribution, and reproduction in any medium, provided the original work is properly cited. For commercial re-use, please contact journals.permissions@oup.com

GRAPHICAL ABSTRACT

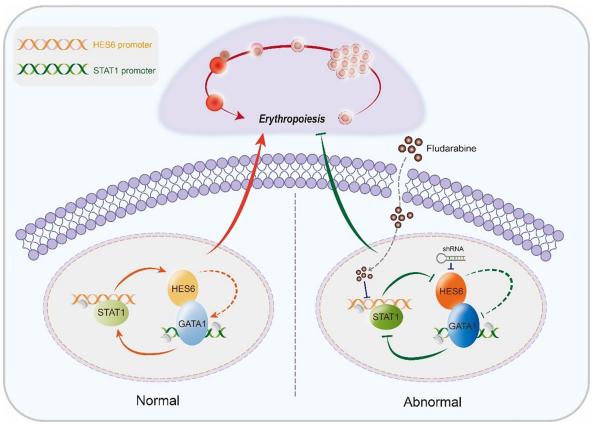

INTRODUCTION

Human erythropoiesis is the process by which hematopoietic stem cells (HSCs) first commit to burst-forming unit-erythroid (BFU-E) cells that further differentiate to colony-forming unit-erythroid (CFU-E) cells, which subsequently undergo terminal erythroid differentiation to generate proerythroblasts, basophilic erythroblasts, polychromatic erythroblasts and orthochromatic erythroblasts. Orthochromatic erythroblasts expel their nucleus to generate reticulocytes. Normal erythropoiesis is driven by precise orchestration of specific gene expression at each distinct stage of development (1). Disordered gene expression patterns have contributed to erythroid-related diseases, such as polycythemia vera (PV), an acquired clonal stem cell disease; ∼95% of PV patients harbor the JAK2^{V617F} mutation, which caused a constitutive activation of the erythropoietin (EPO) receptor (EPOR) signaling pathway, leading to uncontrolled erythrocyte proliferation (2). The discovery of novel transcriptional regulatory mechanisms will help to understand normal and disordered erythropoiesis.

Hematopoietic transcription factors (TFs) bind directly to *cis*-regulatory elements to elegantly regulate gene expression by recruiting cofactors that include TATA-binding protein- (TBP) associated factors (TAFs), mediators, chromatin remodelers, histone/protein-modifying enzymes and scaffold proteins to *cis*-regulatory elements, and thus organize the local chromatin structure and coordinate the balance of proximal post-translational modifications necessary for the overall regulation of transcription (3). A series of cofactors have been found to participate in transcription of erythroid genes, such as FOG1 (4), CBP/P300 (5) and LDB1 (6), indicating that normal expression levels and activities of cofactors are critical for orchestrating gene expression patterns during erythropoiesis.

HES6 is a unique member of the family of mammalian homologs of *Drosophila* hairy and enhancer of split (HES). Unlike other HES members, HES6 has been classified as a transcription cofactor, as the loop region within the basic helix–loop–helix (bHLH) domain of HES6 is four or five amino acids shorter than that of other HES proteins and thus cannot bind DNA through its own bHLH domain. It is instead recruited to DNA via interactions with other DNA-binding proteins (7,8). HES6 has been shown to control myogenesis in mouse C2C12 myoblasts and neurogenesis in mouse and *Xenopus* embryos (9,10). However, the regulatory role of HES6 and its interacting TFs in human erythropoiesis remains to be defined.

In this study, we discovered that HES6 was an abundant transcription cofactor at gene level during human erythropoiesis. HES6 is involved in the GATA1–FOG1–NuRD complex and in regulation of GATA1 downstream genes. Chromatin immunoprecipitation (ChIP) and RNA sequencing (RNA-seq) identified motifs, target genes and pathways of GATA1. which involved HES6 cooperation in erythroid cells. Unexpectedly, we found that HES6 and GATA1 reciprocally regulated their transcription via a novel positive feedback loop. HES6 regulated the transcription of *GATA1*. Unexpectedly, GATA1 reciprocally regulated *HES6* transcription by regulating the expression of STAT1. Importantly, this loop is regulated by EPO signaling and up-regulated in CD34$^+$ cells with the JAK2^{V617F} mutation from the PV database. In addition, HES6 knockdown suppressed cell proliferation of erythroid cells in PV patients and JAK2^{V617F} mice. Our findings enabled us to identify a novel regulatory mechanism for human erythropoiesis and potential diagnosis and treatment strategies for PV.

MATERIALS AND METHODS

Blood purification and cell culture

Human cord blood and PV patient bone marrow (BM) samples were obtained from Xiangya Hospital and the Second Xiangya Hospital of Central South University with approval from the Ethics Committees. Informed consent was obtained from all participating subjects. The culture medium composition and culture protocol of cord blood and BM samples to induce CD34$^+$ cells to undergo erythroid differentiation have been described in detail previously (11,12). Briefly, CD34$^+$ cells were purified from cord blood by positive selection using the magnetic-activated cell sorting system (Miltenyi Biotec), according to the manufacturer's instructions. The purity of isolated CD34$^+$ cells was 95–98%. The cell culture procedure was comprised of three phases. the cells were cultured in Iscove's modified Dulbecco's medium (IMDM, Life Technologies) containing 2% human AB plasma, 3% human AB serum, 200 μg/ml human holo-transferrin, 3 IU/ml heparin, 10 μg/ml insulin and 1% penicillin/streptomycin. In Phase I (day 0–6), CD34$^+$ cells at a concentration of 10^5/ml were supplemented with 10 ng/ml stem cell factor (SCF), 1 ng/ml interleukin 3 (IL-3) and 3 IU/ml EPO. In Phase II (day 7–11), the cells were supplemented with 1 IU/ml EPO and 10 ng/ml SCF alone. In Phase III (day 12–21), the cell concentration was adjusted to 10^6/ml on day 11 and to 5×10^6/ml on day 15. The medium for this phase was the base medium containing 1 IU/ml EPO and 1 mg/ml holo-transferrin. The cells were cultured at 37°C in the presence of 5% CO_2, and were split into fresh culture medium every 3 days. HEK293T cells (ATCC® CRL-11268™) were cultured in Dulbecco's modified Eagle's medium (DMEM) (Gibco, NY, USA) supplemented with 10% fetal bovine serum (FBS) (Gibco). The HEL cell line with JAK2^{V617F} mutation (13) was authenticated by Sanger sequencing (Supplementary Figure S7D),

and cultured in RIPM (Gibco) supplemented with 10% FBS (Gibco).

Virus infection

A total of 30 million lentiviruses were used to infect 0.5 million primary erythroid cells on day 2. At 14 h after infection, cells were washed with phosphate-buffered saline (PBS) and cultured in new complete medium. At 48 h after infection (day 4), cells were selected with 1 μg/ml puromycin until the end of the culture period. For GATA1 rescue assay, 0.5 million cultured primary erythroid cells were infected with 40 million HES6 short hairpin RNA (shRNA) or control shRNA lentivirus on day 2 of culture with a multiplicity of infection (MOI) of 80 and, on day 7, cells were again transduced with either 30 million control or GATA1-overexpressing lentivirus with an MOI of 80. Starting at day 9, the extent of terminal erythroid differentiation was monitored.

Nucleoprotein extraction and identification of HES6-interacting partners

A total of 1×10^7 cultured primary erythroid cells at day 2 were infected with lentiviruses expressing pLV-3*FLAG-HA-HES6 or pLV-3*FLAG-HA vectors with an MOI of 80. At 48 h after infection, cells were selected with 1 μg/ml puromycin. At day 9, nuclear extracts were collected using the NE-PER™ Nuclear and Cytoplasmic Extraction Kit (Thermo Scientific™, #PI78833). Briefly, cells were harvested and then centrifuged at 500 *g* for 5 min. After washing with ice-cold 1× PBS, 200 μl of ice-cold hypotonic buffer [10 mM HEPES, 1.5 mM $MgCl_2$, 10 mM KCl, 0.5 mM dithiothreitol (DTT), 1 mM EDTA, pH 7.9] containing 1× protease inhibitor cocktail (Sigma-Aldrich, P8849) was added to burst the cell pellet, and incubation was carried out on ice for 10 min. Then, 11 μl of ice-cold detergent (0.05% NP-40) was added, and the incubation was prolonged on ice for an additional 1 min. After centrifugation (5 min at 16 000 *g*), the supernatant (cytoplasmic extract) was transferred to a pre-chilled tube while the pellet fraction containing the nuclei was suspended in 100 μl of ice-cold nuclear extraction buffer (5 mM HEPES, 1.5 mM $MgCl_2$, 300 mM NaCl, 0.2 mM EDTA, 0.5 mM DTT, 26% glycerol, pH 7.9) containing 1× protease inhibitor cocktail. The samples were placed on ice and vortexed for 15 s every 10 min for a total of 40 min. After centrifugation (10 min at 16 000 *g*), the supernatant (nuclear extract) was collected into a pre-chilled tube.

A FLAG® HA Tandem Affinity Purification Kit (Sigma-Aldrich, MO, USA, #TP0010) was then used to detect interactors of HES6 in nuclear extracts following the manufacturer's protocol. Briefly, the nuclear extract was incubated with anti-FLAG M2 resin rotating overnight at 4°C. The supernatant was then removed, and the resin was washed with RIPA buffer (Sigma, R0278) containing protease inhibitors. The first elution of the protein complex bound on the resin was done by using 3*FLAG peptide, and in a following step the eluate was bound to anti-HA resin slurry. In the second elution of the protein complex, the anti-HA slurry was washed with Tris-buffered saline (TBS; 0.138 M NaCl, 0.003 M KCl, 0.05 M Tris, pH 8.0) to remove unbound proteins. The final elution was done by using TBS with 100 mM ammonium bicarbonate, and the sample was subsequently resolved by 10% sodium dodecylsulfate–polyacrylamide gel electrophoresis (SDS–PAGE). Specific protein bands of the experimental group on silver-stained gels were excised and analyzed by liquid chromatography–tandem mass spectrometry (LC-MS/MS) (14).

DNA pull-down

Promoter DNA that was labeled with biotin in the 5′-flanking region was cloned from recombinant plasmids containing the gene-specific promoter sequence or mutant promoter sequence by polymerase chain reaction (PCR) amplification. The biotin-scrambled DNA that has the same sequence length as the promoter sequence in the experimental group served as a negative control. Following DNA purification (Qiagen, #28104), biotin-tagged promoter DNA (5 μg) was mixed with nuclear extracts isolated from human erythroid cells (500 μg) at day 9 using the NE-PER™ Nuclear and Cytoplasmic Extraction Kit and 100 μl of streptavidin-coupled Dynabeads (Thermo Fisher Scientific, MA, USA) in binding buffer (50 mM Tris–HCl, pH 8.0 and 150 mM NaCl, 1% Triton X-100 and 1 mM phenylmethylsulfonyl fluoride) and incubated at 4°C overnight. Following incubation, the precipitated complexes were washed three times with the wash buffer (0.5 M NaCl, 20 mM Tris pH 7.5, 1 mM EDTA). A 20 μl aliquot of binding proteins was then denatured and subjected to LC-MS/MS analysis or western blotting assay.

Chromatin immunoprecipitation sequencing (ChIP-seq) and data processing

ChIP assay was performed with the Pierce™ Magnetic ChIP Kit (Thermo Fisher Scientific) according to the manufacturer's protocol. Briefly, a total of 1×10^7 erythroid cells at day 2 were transfected with lentiviruses expressing pLV-3*FLAG-GATA1-HA or pLV-3*FLAG-HES6-HA with a MOI of 80. Following differentiation for 7 days, 4×10^6 cells for each group were harvested, fixed with 1% formaldehyde for 10 min and quenched with 0.125 M glycine for 5 min. Chromatin was isolated, digested by micrococcal nuclease (MNase), sheared by sonication and immunoprecipitated with ChIP-grade FLAG or ChIP-grade rabbit IgG antibodies (other ChIP-grade antibodies are shown in the antibody list of Supplementary Data). Immunoprecipitated DNA was washed and eluted according to the manufacturer's instructions. DNA was then purified using column-based DNA purification kits (Sangon Biotech Co., Shanghai, China, #B110093-0100). Purified DNA was analyzed by quantitative reverse transcription–PCR (qRT–PCR) or subjected to the ChIP-seq that was performed by the Novogene Corporation (Beijing, China). The primers are shown in the primer list of Supplementary Data.

For data processing, PCR products were purified (AMPure XP system) and library quality was assessed on the Agilent Bioanalyzer 2100 system. The library preparations were sequenced on an Illumina Hiseq platform and 150 bp paired-end reads were generated. Then, the raw reads

were cleaned by Trim_galore and aligned to the reference human genome (UCSC hg38) using Hisat2. Duplicate and multi-mapped reads were removed using the markdup command of Sambamba. The ChIP-seq data were normalized to RPGC (number of reads per bin/scaling factor for 1× average coverage) and significant peaks were identified using MACS2 with a *P*-value ≤0.001. The ChIP-seq read density plot and heatmap were generated by deepTools. All motif analysis was done with the HOMER v4.7.2. software35 (http://homer.salk.edu/homer), using default parameters. The ChIP-seq data have been deposited in the National Genomics Data Center (https://ngdc.cncb.ac.cn/?_blank) with the dataset identifier PRJCA011578.

Transcriptome analysis

RNA was extracted from erythroblasts infected with lentivirus containing control shRNA or human HES6 shRNA-2 at day 9, and was subjected to the RNA-seq that was performed by the Novogene Corporation (Beijing, China). Libraries were prepared using the RNA Nano 6000 Assay Kit of the Bioanalyzer 2100 system and sequenced on an Illumina NovaSeq 6000. The 150 bp pair-end reads were generated for each sample. Raw data were filtered by Trim_galore for quality control and mapped to the human (UCSC hg38) genome by Hisat2. Gene expression and differentially expressed genes (DEGs) were estimated by the Limma package. Data representation and statistics were conducted in R. Principal component analysis (PCA) was performed on expressed genes in control and shRNA groups [fragments per kilobase of transcript per million mapped reads (FPKM) ≥0.1 in at least two samples]. Gene set enrichment analysis (GSEA) was performed using the R package 'clusterProfiler'. Pathway analysis was performed using the Reactome database. Gene Ontology (GO) enrichment analyses were performed using DAVID (https://david.ncifcrf.gov/home.jsp). The RNA-seq data have been deposited in the National Genomics Data Center (https://ngdc.cncb.ac.cn/?_blank) with the dataset identifier PRJCA011578.

Knockdown of HES6 by CRISPR-HES6 sgRNA

Single-guide RNAs (sgRNAs) targeting the human HES6 gene sequences are: sgRNA-1, 5′-GCGAGCGAGCGCTTCGCTGC-3′; and sgRNA-2, 5′-GGACGACCTGTGCTCCGACC-3′. Oligonucleotides were cloned into the lentiviral vector lentiCRISPR v2 (Addgene, # 52961). HEL cells were incubated with lentiviruses for 12 h before washing away the excess virus. After 48 h infection, cells were selected with 1 μg/ml puromycin for 1 week and then used for further experiments.

Statistical analysis

The significance of the differences between the control and the experimental groups was evaluated by Student's *t*-test using SPSS 18.0 statistical software. Values are shown as the mean ± standard deviation (SD) for three independent experiments. One-way analysis of variance and Fisher's least significant difference test were performed with GraphPad Prism 7.0 (GraphPad software) and were used to compare different groups from the GEP dataset. The correlation analysis was performed using Pearson's correlation test. $P < 0.05$ was considered statistically significant.

RESULTS

HES6 positively regulates human erythropoiesis

In order to define the potential contribution of transcription cofactors to human erythropoiesis, we analyzed their expression patterns during erythropoiesis using our published RNA-seq data (15). As shown in Figure 1A and Supplementary Table S1, 418 transcription cofactors, including TAFs, mediators, chromatin remodeling factors, histone/protein-modifying enzymes and scaffold proteins, were found to be expressed in erythroid cells. Among them, HES6 was expressed at high gene levels. Compared with another nine HES family/superfamily members, only HES6 was highly expressed in erythroid cells and its expression increased during erythroid differentiation (Supplementary Figure S1A). This pattern of expression was further confirmed by qRT–PCR (Figure 1B) and by western blotting (Figure 1C). HES6 also exhibited higher gene expression levels than some other established erythroid TFs and cofactors, such as Trim28 (16), TAF9 (17), KLF1 (18) and TAL1 (19) (Supplementary Figure S1B). To study the role of HES6 in human erythropoiesis, we used the shRNA-mediated knockdown approach with $CD34^+$ cells. HES6 was efficiently down-regulated by two independent shRNAs (Supplementary Figure S1C). shRNA specificity was validated by using both loss-of-function experimental strategies and rescue with HES6 overexpression (Supplementary Figure S1D–F). HES6 knockdown markedly decreased erythroid colony formation and has a mild influence on granulocyte–macrophage (GM) colony formation, but no impact on multilineage myeloid progenitor cells (GEMM; Figure 1D), implying a role for HES6 in committed erythroid progenitors. Further, HES6 knockdown inhibited growth of terminal erythroid cells, causing a high degree of apoptosis (Figure 1E; Supplementary Figure S1G), and delaying cell differentiation, as reflected by the delayed expression of Glycophorin A (GPA)(Figure 1F; Supplementary Figure S1H) as well as a lag in the down-regulation of α4-integrin expression and up-regulation of band 3 expression (Figure 1G, H). A delay in enucleation was also noted following HES6 knockdown (Supplementary Figure S1I). These findings imply an important role for HES6 in human erythropoiesis.

HES6 is a binding partner of the GATA1-NURD complex

To define the mechanisms by which HES6 regulates erythropoiesis, we sought to identify potential TF binding partners of HES6. We transfected 3× Flag-HA-tagged HES6 cDNA into cultured human erythroblasts at day 2 and performed 3× Flag-HA tandem affinity purification using nuclear extracts in conjunction with LC-MS/MS analysis for protein identification at day 9 (Figure 2A; Supplementary Table S2). The putative TF binding partners were screened

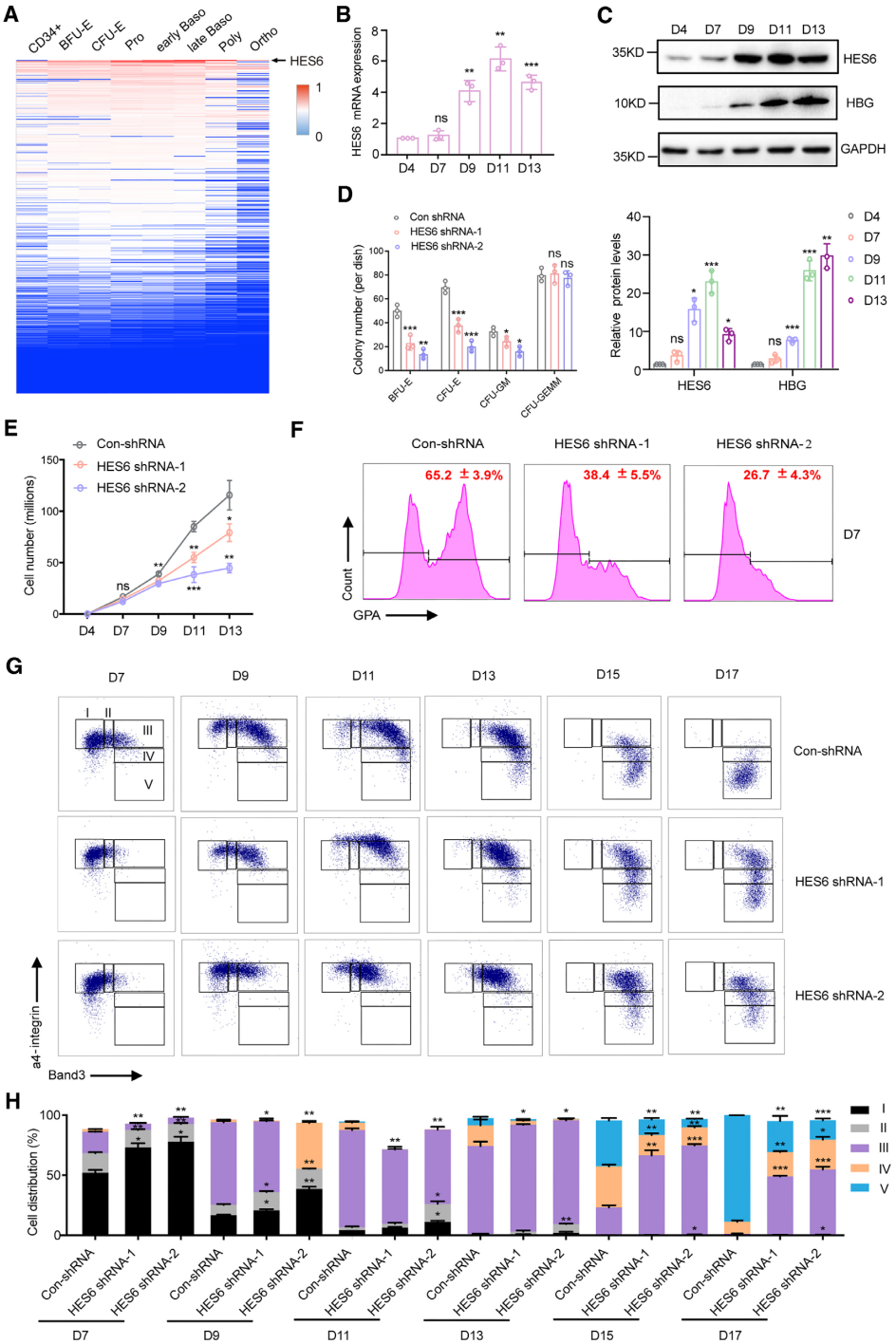

Figure 1. HES6 positively regulates human erythropoiesis. (**A**) Heatmap showing mRNA expression levels of 418 transcription cofactors at each developmental stage of human erythroid differentiation using a public RNA-seq database. BFU-E, burst-forming unit-erythroid; CFU-E, colony-forming unit-erythroid; Pro, proerythroblast; Baso, basophilic erythroblast; Poly, polychromatic erythroblast; Ortho, orthochromatic erythroblast. (**B**) qRT–PCR results showing HES6 expression at each developmental stage of human erythroid differentiation [day 4 (D4), BFU-E; D7, Pro; D9, Baso; D11, Poly; D13, Ortho]. The results were normalized to glyceraldehyde phosphate dehydrogenase (GAPDH) mRNA expression levels. (**C**) Western blotting analysis of HES6 expression at each developmental stage of human terminal erythroid differentiation. GAPDH was used as a loading control. Densitometric analysis of protein levels used ImageJ software. Statistical analyses of $n = 3$ independent experiments were performed (bottom). (**D**) The number of BFU-E, CFU-E, CFU-GM and CFU-GEMM colonies derived from $CD34^+$ HSCs infected with control shRNA or HES6 shRNA were counted manually. (**E**) Erythroid cell growth curves determined by manual cell counting of erythroblasts infected with control shRNA or HES6 shRNA. (**F**) Representative images of flow cytometry analysis of GPA expression in erythroblasts infected with control shRNA or HES6 shRNA on day 7. Statistical analysis of the GPA-positive cells from three independent experiments are shown. (**G**) Representative images of the flow cytometry analysis of band 3 and α4-integrin expression on D7, D9, D11, D13, D15 and D17 of GPA-positive erythroblasts infected with control shRNA or HES6 shRNA. (**H**) The cell distribution analysis based on the flow cytometry results from erythroblasts infected with control shRNA or HES6 shRNA. Statistical analysis of the data was from three independent experiments, and the bar plot represents the mean ± SD of triplicate samples. $^*P < 0.05$, $^{**}P < 0.01$, $^{***}P < 0.001$ versus control based on Student's *t*-test.

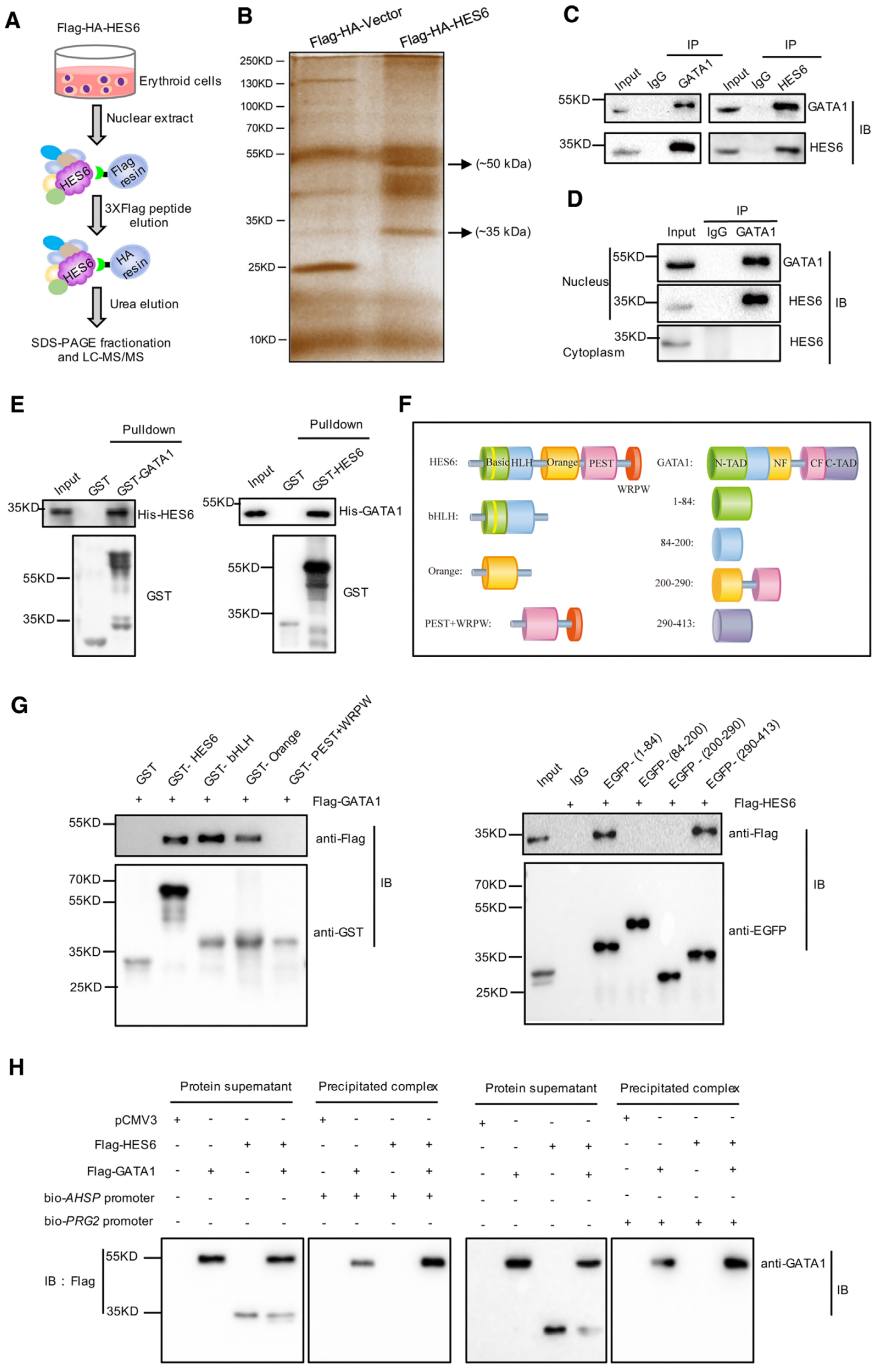

Figure 2. GATA1 is a binding partner of HES6 in human erythroid cells. (**A**) Schematic representation of the FLAG-HA tandem affinity purification process. (**B**) A representative image of a whole silver-stained gel of precipitated protein complex samples following FLAG-HA-HES6 tandem affinity purification. Specific bands containing GATA1 protein (∼50 kDa) and HES6 protein (∼35 kDa) are indicated by the arrows. The negative control is cultured human erythroblasts transfected with empty Flag-HA vector (pLV-3*FLAG-HA vector). (**C**) Co-IP results showed that GATA1 or HES6 was immunoprecipitated from primary erythrocyte lysates (at day 9) with an anti-GATA1 or anti-HES6 antibody. GATA1 or HES6 in the immunoprecipitate was detected with an anti-GATA1 or anti-HES6 antibody, respectively. (**D**) Co-IP results confirmed that the HES6 and GATA1 interaction occurred in the nucleus but not in the cytoplasm. Total proteins were used as a positive input control. (**E**) Representative western blotting analysis of the pull-down assay using purified GST–GATA1 with purified His-HES6, and purified GST–HES6 with purified His-GATA1. (**F**) Schematic diagram showing the functional domains of HES6 and GATA1, respectively. The HES6 protein includes a bHLH, Orange, PEST and WRPW domain. The GATA1 protein includes N-terminal (N-TAD) and C-terminal (C-TAD) domains and two zinc finger (NF and CF) domains located in the middle of the molecule. (**G**) Left panel: purified GST–HES6 deletion mutants were incubated with HEK293T cell lysates expressing Flag-tagged GATA1, and their interactions were analyzed using a pull-down assay. Right panel: EGFP-tagged GATA1 deletion mutants and Flag-tagged HES6 were co-transfected into HEK293T cells. Their interactions were analyzed using a Co-IP assay. (**H**) Under conditions of equivalent amounts of transfected plasmids and streptavidin-coupled Dynabeads, the DNA pull-down assay was used to evaluate the alteration in interactions between exogenous Flag-GATA1 and bio-*AHSP* (left panel) and bio-*PRG2* (right panel) promoter DNA in the presence or absence of exogenous Flag-HES6. The expression of Flag-HES6 and Flag-GATA1 in protein supernatants served as loading controls. The empty pCMV3-C-flag vector was used as a negative control.

based on the following criteria: (i) the –10log *P*-value (referred to as the protein confidence score) and (ii) comparable expression of HES6 and the TFs. Based on these criteria, GATA1 was identified as a potential HES6-interacting TF (Figure 2B; Supplementary Figure S2A–D). To determine if HES6 and GATA1 interact, we performed a co-immunoprecipitation (Co-IP) assay using total cell, nuclear and cytoplasmic lysates of cultured primary human erythroblasts. As shown in Figure 2C, there is reciprocal Co-IP of GATA1 and HES6, specifically, in the nuclear fractions (Figure 2D). To further validate direct binding of HES6 to GATA1, we performed a glutathione *S*-transferase (GST) pull-down assay. As shown in Figure 2E, purified GST–GATA1, but not the control GST, was able to pull-down His-HES6. Similarly, purified GST–HES6, but not the control GST, brought down His-GATA1. To further define the specific domains of HES6 and GATA1 involved in the interaction, recombinant proteins representing the GST-tagged functional domains of HES6 and enhanced green fluorescent protein (EGFP)-tagged functional domains of GATA1 were generated as shown in Figure 2F. Pull-down assays using the recombinant proteins showed that the bHLH domain and Orange domain of HES6 and the N- and C-terminal transactivation domains (N-TAD and C-TAD) of GATA1 were involved in the interaction between HES6 and GATA1 (Figure 2G).

To further explore in which GATA1 complex HES6 participates, we analyzed the LC-MS/MS data; some components of the GATA1–NuRD complex were also identified, including HDAC1, HDAC2, MTA2, RBBP4 and RBBP7 (Supplementary Table S2). We firstly confirmed that GATA1 was able to interact with GATA1–NuRD complex components, including CHD3, CHD4, FOG1, MTA1, HDAC1, HDAC2, RBBP7 and MBD3 in erythroid cells by Co-IP assay. Correspondingly, HES6 also interacted with these components, which indicates that HES6 participates in the GATA1–NuRD complex (Supplementary Figure S3A, B). In particular, through the quantitative Co-IP assay, we found that the number of FOG1 pulled down by an equal quantity of GATA1 was significantly decreased upon HES6 knockdown. This suggests that HES6 plays an important role in stabilizing the GATA1–FOG1–NuRD complex (Supplementary Figure S3C).

HES6 enhances GATA1 transcriptional activity by facilitating its DNA binding occupancy

Cofactors regulate gene transcription by affecting the transcriptional activity of TFs (20). Having shown that HES6 interacted with transactivation domains of GATA1, we explored the effect of HES6 on GATA1 transcription activity using luciferase reporter assay. Two commonly used GATA1 target genes, α-hemoglobin-stabilizing protein (*AHSP*) and proteoglycan 2 (*PRG2*), were chosen for this study (21,22). As shown in Supplementary Figure S2E, compared with the groups ransfected with GATA1 or HES6 alone, the GATA1 plus HES6-co-transfected group showed strong fluorescence activity for both *AHSP* and *PRG2* genes, implying HES6 enhancement of GATA1 transcription activity. Given that HES6 is a non-enzymatic cofactor without the ability to modify interacting TFs, we reasoned that HES6 might regulate GATA1 transcriptional activity by affecting its DNA binding occupancy. To test this, we performed a DNA pull-down assay to examine the effect of HES6 on the binding of GATA1 to its target gene promoter. As shown in Figure 2H, HES6 increased the binding events of GATA1 to both *AHSP* and *PRG2* promoters, validating a functional interaction between HES6 and GATA1.

HES6 promotes erythropoiesis through the transcriptional regulation of GATA1

In order to determine if HES6 regulates human erythropoiesis through GATA1, a rescue strategy was adopted. Since it has been shown that transcription cofactors regulate TF expression by either regulating their transcription or altering protein stability (20), we firstly examined the effect of HES6 deficiency on GATA1 expression. Notably, HES6 knockdown led to decreased expression of GATA1 as well as the GATA1 downstream target 4.1R at both protein and mRNA levels (Figure 3A, B), but had little effect on some other erythroid TFs (Supplementary Figure S4A, B). For GATA1 rescue assay, unexpectedly, we found that ectopic expression of GATA1 at near normal intracellular levels not only rescued the expression of HES6 at both mRNA and protein levels in HES6-knockdown erythroid cells (Figure 3C, D), but also rescued the delayed differentiation (Figure 3E, F; Supplementary Figure S4C), and impaired cell growth (Figure 3G) and cell apoptosis (Supplementary Figure S4D) of HES6-knockdown erythroid cells. These results suggest that HES6 modulates human erythropoiesis by regulating the transcription of GATA1, and GATA1 reciprocally regulates the expression of HES6.

Integration of ChIP-seq and RNA-seq reveals a rich set of HES6- and GATA1-co-regulated genes

Since HES6 directly interacted with GATA1, we then investigated the downstream co-regulatory mechanisms of HES6 and GATA1. We firstly examined the global transcriptional effect of HES6 knockdown; RNA-seq assays were performed on erythroblasts infected with control shRNA or HES6 shRNA vectors on day 9 of culture. A total of 2551 genes comprising 1535 up-regulated genes and 1016 down-regulated genes were significantly changed upon HES6 knockdown ($|\log FC| > 0.5$; $P < 0.05$), including a series of cell cycle- and/or apoptosis-related molecules (Figure 4A). GSEA revealed that those altered genes are functionally related to developmental process, cell growth and apoptosis regulation (Figure 4B). For example, the p53-regulated transcription of cell death genes was significantly enriched in apoptosis regulation process (Figure 4C). Five candidate genes: TP53INP1, p73, CREBBP, TRIAP1 and PRELID1, were selected for further validation by qRT–PCR using material from the independent set of experiments (Figure 4D).

To identify genome-wide binding sites of GATA1 and HES6, ChIP-seq assays were performed on erythroblasts infected with 3× Flag-HES6 or 3× Flag-GATA1 vectors on day 9 of culture. With values normalized to the input, we identified 7274 HES6 binding peaks and 1535 GATA1 binding peaks. Notably, the number of overlapping peaks is 1362 (Figure 4E), which suggests that HES6 acting as a

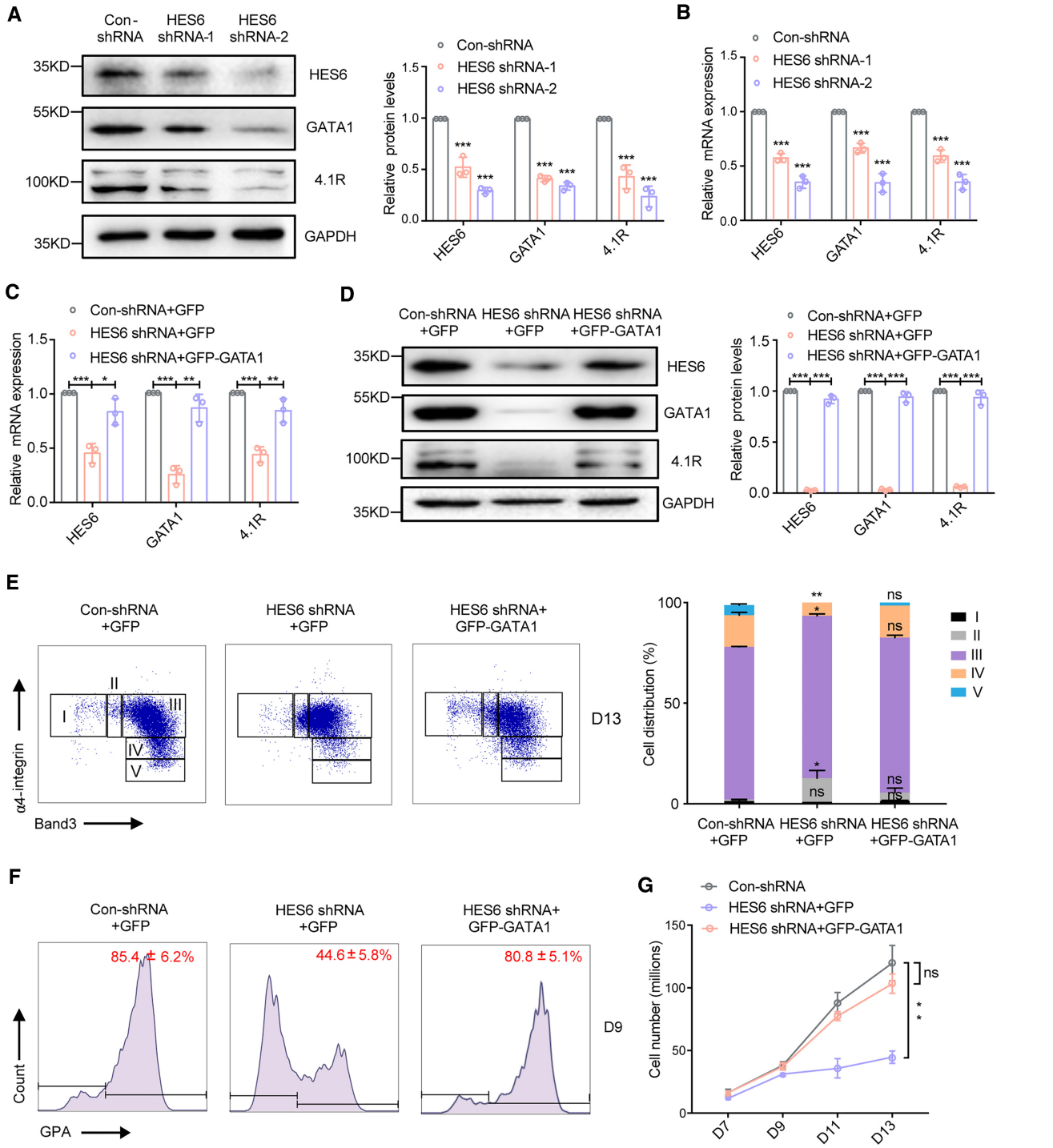

Figure 3. HES6 promotes human erythropoiesis through the transcriptional regulation of GATA1. (**A**) Representative images of western blotting analysis showing HES6, GATA1 and 4.1R expression in erythroblasts infected with lentivirus containing control shRNA or HES6 shRNA. Right panel: quantitative analysis of protein expression data from three independent experiments. GAPDH was used as a loading control. (**B**) qRT–PCR analysis showing HES6, GATA1 and 4.1R expression levels in erythroblasts infected with lentivirus containing control shRNA or HES6 shRNA on day 9 of culture. The results were normalized to GAPDH mRNA. (C and D) Cultured primary erythroblasts co-infected with control shRNA plus HMD–GFP vectors, HES6 shRNA plus HMD–GFP vectors and HES6 shRNA plus non-fused HMD–GATA1–GFP overexpression vectors on day 9. qRT–PCR (**C**) and western blotting (**D**) analysis of the mRNA and protein levels of HES6, GATA1 and 4.1R. HMD–GATA1–GFP was expressed at levels comparable with those of wild-type GATA1. Quantitative analysis of protein expression data from three independent experiments is shown. (E and F) Representative flow cytometry data for erythroblasts co-infected with the same amount of plasmids as indicated in (D). Expression of band 3 and α4-integrin was monitored on day 13 (**E**) and GPA expression was monitored on D9 (**F**). Statistical analysis of the GPA-positive rate and cell distribution (%) from three independent experiments is shown. (**G**) Erythroid cell growth curves determined by manual cell counting of erythroblasts following co-infection with the same amount of plasmids as indicated in (D). Statistical analysis of the data from three independent experiments; the bar plot represents the mean ± SD of triplicate samples. *P <0.05, **P <0.01, ***P <0.001 versus control based on Student's t-test.

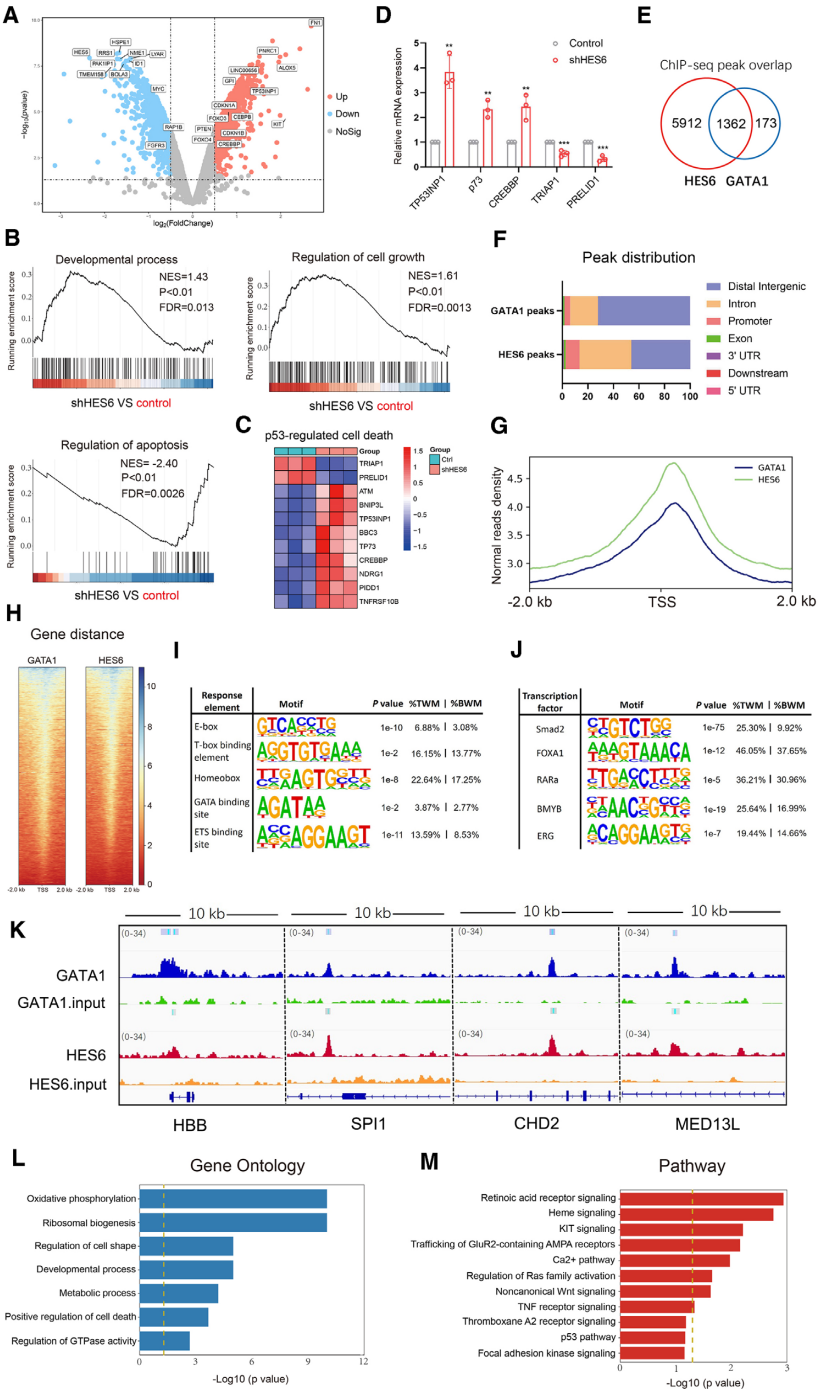

Figure 4. ChIP-seq and RNA-seq analysis of HES6- and GATA1-co-regulated genes. (**A**) Volcano plot of DEGs in RNA-seq of HES6 knockdown. Red dots represent significantly up-regulated genes (|logFC| >0.5; P <0.05); blue dots represent significantly down-regulated genes (|logFC| >0.5; P <0.05); and black dots (NO) represent DEGs below the level of significance. (**B**) GSEA of DEGs of RNA-seq data of HES6 knockdown. Developmental process, cell growth and apoptosis regulation gene sets are significantly enriched in the HES6 knockdown group. (**C**) Example of the apoptosis regulation process showing that p53-regulated transcription of cell death genes was enriched. (**D**) Five candidate genes selected from (C) were validated by qRT–PCR using material from the independent set of experiments. (**E**) Venn diagram showing the overlap of HES6 and GATA1 downstream target genes. (**F**) Genomic distribution of HES6 and GATA1 ChIP-seq peaks. (**G**) Averaged profiles of HES6 (green) and GATA1 (blue) ChIP-seq reads centered on the transcription start site (TSS) (±2 kb). (**H**) Heatmaps of normalized density of HES6 and GATA1 ChIP-seq tags centered on their binding peaks across a ± 2 kb window. The color key represents the signal density. (**I**) Motif enrichment analysis of HES6- and GATA1-co-bound promoter peaks, listing motifs from five significantly enriched response elements. (**J**) Motif enrichment analysis of co-bound promoter peaks of HES6 and GATA1, listing the top five enriched motifs. TFs potentially recognizing the motifs are displayed. %TWM, percentage of targets with motif; %BWM, percentage of background with motif. (**K**) Genome browser views of 10 kb genomic loci of the indicated genes (HBB, SPI1, CHD2 and MED13L) depicting ChIP-seq tracks with called peaks (gray bars) for HES6 and GATA1. Bars over peaks indicate significantly bound peaks with a cut-off q-value of 0.05. Input acts as a negative control. (L and M) GO term enrichment (**L**) and Reactome pathway (**M**) analysis of co-regulated genes of HES6 and GATA1. Top up- and down-regulated GO terms and pathways are shown.

transcriptional cofactor was present at a majority of target genes of GATA1. Analysis of all peaks revealed that the majority of HES6 and GATA1 peaks resided within distal intergenic regions (46.1% for HES6, 72.1% for GATA1), and other fractions were present at either intron regions (40.4% for HES6, 21.6% for GATA1) or promoters (10.8% for HES6, 4.7% for GATA1) (Figure 4F). The overlapping regions between HES6 and GATA1 are observed around the transcription start site (TSS) (Figure 4G). Correspondingly, the heatmap analysis showed that the peak densities of HES6 and GATA1 were also enriched within elements ± 2 kb proximal to the TSS (Figure 4H). Next, using Homer for *de novo* motif discovery in the HES6 and GATA1 co-binding sites, we identified enrichment of some response elements, including an E-box motif, a T-box binding element (TBE), a NKX3.2 Homeobox, a GATA-binding site and an ETS motif (Figure 4I). Strikingly, these DNA elements previously were shown to be associated with GATA1 function (23). We also found that the co-binding motifs of HES6 and GATA1 are the most significant motif found in Smad2-, FOXA1-, Retinoic acid receptor alpha (RARα)-, BMYB- and ERG-bound regions, suggesting a possible TF cooperativity at promoter sites in regulating target genes (Figure 4J).

We next performed an integrated analysis of the ChIP-seq and RNA-seq data. Among co-regulated genes, we found that 263 co-regulated genes were modulated significantly upon HES6 knockdown ($|\log FC| > 0.5$; $P < 0.05$), including HBB, SPI1, CHD2 and MED13L, all of which were previously suggested to be direct GATA1 targets (Figure 4K). GO enrichment analysis revealed that these co-regulated genes were primarily involved in regulation of cell shape and death, regulation of GTPase activity, oxidative phosphorylation, developmental process, metabolic process, ribosomal biogenesis, etc. (Figure 4L). Pathway analysis showed that these genes participate in a series of erythroid-related pathways, including KIT, GluR2-AMPA, calcium (Ca^{2+}), RARs, RAS, non-canonical Wnt, tumor necrosis factor (TNF) receptor, thromboxane A2 (TXA2) receptor, p53, focal adhesion, heme signaling, etc. (Figure 4M). Together, these results suggest that GATA1 works on the genome at least through cooperation with HES6, which regulates the expression of multiple erythroid-related biological processes and pathways.

GATA1 positively regulates *HES6* transcription via the transcription factor STAT1

We previously found that ectopic expression of GATA1 in HES6-knockdown erythroblasts restored HES6 expression (Figure 3C, D). We further knocked down GATA1 by short interfering RNA (siRNA) and found that GATA1 knockdown indeed led to decreased gene and protein expression of HES6 (Figure 5A; Supplementary Figure S5A), which strongly implies that GATA1 reciprocally regulates HES6 expression. To explore the underlying mechanism by which GATA1 transcribes the HES6 gene, we first analyzed the ChIP-seq data for GATA1. However, analysis of our GATA1 ChIP databases or public GATA1 ChIP databases (ENCODE: GSM 970258, 722392, 1067274) failed to identify GATA1 binding peaks on the *HES6* promoter and distal regulatory region (within 30 kb upstream from the TSS) in human erythroid cells (Supplementary Figure S5B). Furthermore, data from *in vitro* DNA pull-down assay also show that GATA1 could not bind to the upstream 2 kb region of the *HES6* promoter (Figure 5B). To uncover the intermediate TF that mediates the transcriptional regulatory role of GATA1 on *HES6*, we performed a DNA pull-down assay using the *HES6* promoter including the 2 kb to +200 bp region (Supplementary Table S3). As shown in Figure 5C, a 90 kDa protein was pulled down by the *HES6* promoter but not by the scrambled DNA fragment. STAT1 was identified as a potential upstream *HES6* TF, which has: (i) a high –10log *P*-value; (ii) a similar expression pattern to *HES6*; and (iii) positive changes in gene expression following alteration of GATA1 (Figure 5D; Supplementary Figure S5C–E).

We then examined whether STAT1 directly regulates *HES6* transcription. Using an siRNA-mediated STAT1 knockdown strategy, we found that STAT1 positively regulates the gene and protein expression of HES6 (Figure 5E; Supplementary Figure S5F). Further, the public ChIP database (CistromeDB: 41289) and JASPAR database revealed that there are STAT1 binding peaks on the *HES6* promoter region (–437 bp to +92 bp from the TSS), which includies a STAT1 binding site 'GGGACCTGAAACCC' (Supplementary Figure S5G). ChIP-qPCR confirmed that two DNA fragments (–244 to –377 and –185 to –296) containing a HES6 peak region could be pulled down by STAT1 protein (Figure 5F). *In vitro* DNA pull-down assay also showed that STAT1 could directly bind to the *HES6* promoter including the –437 to +92 sequence, but not the promoter carrying a mutation at the STAT1 binding site (Figure 5G). Thus, STAT1 can activate *HES6* gene expression via direct binding to its promoter. Further, we examined the effect of GATA1 on the transcription of *STAT1*. GATA1 overexpression increased the transcription of *STAT1* and *HES6*, accompanied by increased levels of protein expression (Figure 5H; Supplementary Figure S5H). To further demonstrate that GATA1 regulates *STAT1* transcription directly, we comprehensively analyzed the public ChIP database (CistromeDB: 33545), GATA1 ChIP-seq and the JASPAR database. A GATA1 peak region on the *STAT1* promoter (–366 to –47 from the TSS) that contains a GATA1 binding site 'GCCAAATCTGT' in human erythroid cells (Supplementary Figure S5I, J) was found. The ChIP-qPCR confirmed that ChIP-grade GATA1 antibody could pull down the endogenous *STAT1* promoter fragments (–190 to –335 and –212 to –315) in erythroblasts (Figure 5I). DNA pull-down assay showed that *STAT1* promoter DNA including –366 to –47 upstream sequence was able to pull down GATA1 protein, but not the promoter carrying a mutation in the GATA1 binding site *in vitro* (Figure 5J). These findings imply that GATA1 regulates *STAT1* transcription by directly binding to the *STAT1* promoter (Figure 5K).

EPO/EPOR–JAK2^{V617F} signaling promotes expression levels of HES6–GATA1 loop components in PV patients

Our findings imply that HES6 and GATA1 form a positive feedback loop composed of HES6, GATA1 and STAT1.

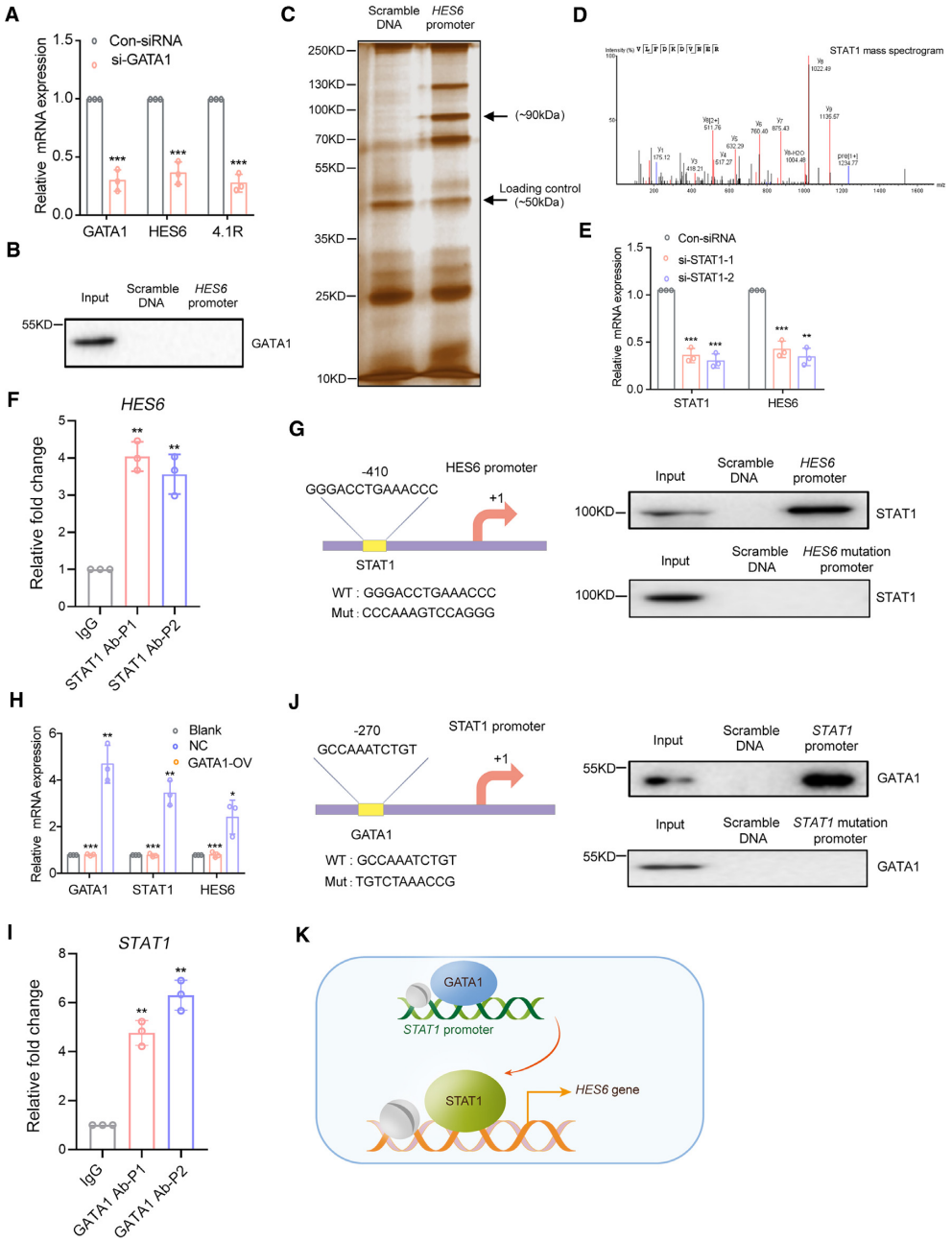

Figure 5. GATA1 positively regulates *HES6* transcription via the TF STAT1. (**A**) qRT–PCR analysis of GATA1, HES6 and 4.1R mRNA levels in cultured primary erythroblasts transfected with control siRNA or GATA1 siRNA at day 9. The results were normalized to GAPDH mRNA. (**B**) Western blotting analysis showing that GATA1 protein cannot be pulled down by the bio-*HES6* promoter DNA (–2 kb to + 200 bp). The negative control is the biotin-tagged scramble DNA that has the same sequence length as the promoter sequence. (**C**) A representative image of a whole silver-stained gel of precipitated protein samples pulled down by the biotin-*HES6* promoter DNA. The specific band containing STAT1 (~90 kDa) is marked with an arrow. The ~50 kDa band acted as a loading control. (**D**) The STAT1 mass spectrogram and its specific amino acid sequence used for identification of the protein from the protein database are shown. (**E**) qRT–PCR analysis of STAT1 and HES6 mRNA levels in erythroblasts transfected with control siRNA or STAT1 siRNA at day 9. (**F**) Graphs showing ChIP-qPCR amplification of two HES6 promoter fragments pulled down by STAT1 protein using ChIP-grade STAT1 antibody. ChIP-grade IgG antibody was used as a negative control. P1 and P2 primers amplified two HES6 promoter regions (i.e. –244 to –377 and –185 to –296), respectively. (**G**) Western blotting results showing that STAT1 protein could be pulled down by the 580 bp of bio-*HES6* promoter DNA (–462 bp to +118 bp), but not for the mutant promoter DNA. The sequence of the normal site of binding of STAT1 to the *HES6* promoter and its mutant are shown (left panel). (**H**) qRT–PCR analysis of GATA1, STAT1 and HES6 mRNA levels in cultured primary erythroblasts (Blank) and in erythroblasts infected with GATA1 overexpressed or control vector lentivirus at day 9. (**I**) Graphs showing ChIP-qPCR amplification of two STAT1 promoter fragments pulled down by GATA1 protein using ChIP-grade GATA1 antibody. ChIP-grade IgG antibody was used as a negative control. P1 and P2 primers amplified two STAT1 promoter regions (i.e. –190 to –335 and –212 to –315), respectively. (**J**) Western blotting results showing that GATA1 protein could be pulled down by the 370 bp of bio-*STAT1* promoter DNA (–366 bp to –47 bp), but not the mutant promoter DNA. The sequence of the normal site of binding of GATA1 to the *STAT1* promoter and its mutant are shown (left panel). (**K**) Model of the GATA1–STAT1–HES6 transcription regulatory axis in human erythroblasts. Statistical analysis of data from three independent experiments; the bar plot represents the mean ± SD of triplicate samples. **P* <0.05, ***P* <0.01, ****P* <0.001 versus control based on Student's *t*-test.

Components in the HES6–GATA1 regulatory loop can affect each other's expression (Figures 3A, B and 5A, H; Supplementary Figures S5A, F, H and S6). Knowing that STAT1 is involved in EPO signaling (24) and that GATA1 is regulated by EPO signaling (25), we wondered whether EPO can regulate the HES6–GATA1 loop. To test this, we examined the effects of EPO on the expression of different components of the HES6–GATA1 loop. As expected, EPO treatment led to increased expression of HES6, GATA1 and STAT1 at both the mRNA (Figure 6A) and protein expression levels (Figure 6B) in human primary erythroid cells at day 4 in a dose-dependent manner, implying that EPO indeed regulates the HES6–GATA1 loop. Given that PV is characterized by enhanced EPO signaling due to a somatic gain-of-function $JAK2^{V617F}$ mutation in hematopoietic stem cells (26,27), and that EPO increases the expression of HES6–GATA1 loop components, we next examined whether the transcription levels of loop components in BM $CD34^+$ cells is altered in PV patients by analyzing data from public databases (GSE103237). As shown in Figure 6C, the mRNA levels of three loop components were significantly up-regulated in BM $CD34^+$ cells from PV patients, compared with healthy controls, and three loop components were ranked among the top 100 in all up-regulated molecules (Supplementary Figure S7A). Furthermore, there was a positive correlation between the levels of HES6 and other loop components at the mRNA level (Figure 6D).

Enhanced effects of HES6 knockdown and STAT1 inhibition on cell growth of $JAK2^{V617F}$ mutant cells

To explore the potential benefit of targeting the HES6–GATA1 loop in the treatment of PV, we examined the effects of HES6 knockdown, or STAT1 inhibition or in combination on the growth of cells with $JAK2^{V617F}$ mutation. After confirming the presence of genetic modifications on the HES6 gene and that of the HES6–GATA1 loop in $JAK2^{V617F}$ mutant HEL cells upon treatment with two CRISPR-HES6 sgRNAs (Figure 6E, F; Supplementary Figure S8), we showed that either knockdown of HES6 by shRNA or STAT1 inhibition by fludarabine significantly inhibited the growth of HEL cells (Figure 6G). Interestingly, the combination of the two exhibited enhanced anti-growth and pro-apoptosis effects (Supplementary Figure S7B), which was accompanied by the decreased expression of the loop components (Figure 6H). Similar results were obtained from cultured primary erythroblasts from $JAK2^{V617F}$ mutant PV patients (Figure 6I, J; Supplementary Figure S7C). These findings imply that targeting the HES6–GATA1 loop could be a potential therapeutic approach for the management of PV patients.

Hes6 knockdown ameliorates $JAK2^{V617F}$-induced myeloproliferative phenotypes

To further explore the potential benefit of Hes6 in PV treatment *in vivo*, we firstly isolated and purified lineage-negative cells upon Hes6 knockdown from BM of C57BL/6 mice aged 6–8 weeks, and directed them into the erythroid lineage (Figure 7A, B). Consistent with effects in human erythroid cells, Hes6 knockdown inhibited growth of murine erythroid cells (Figure 7C), and delayed erythroid differentiation (Figure 7D). Next, we isolated, purified and amplified c-kit+ cells from BM of $JAK2^{V617F}$ mice, infected with Hes6 shRNA or control shRNA lentivirus, and then transplanted them into lethally irradiated recipient mice ($CD45.1^+$, 6 weeks old). Compared with the control, complete blood counts from Hes6 knockdown-recipient mice at 4, 6 and 8 weeks after transplantation displayed decreased red blood cell (RBC), hemoglobin (HGB), hematocrit (HCT) and red cell distribution width (RDW) (Figure 7E). While the white blood cell (WBC) count and platelets remained unchanged. Hes6 knockdown also moderately reduced splenomegaly (Figure 7F) and total BM cells (Figure 7G). Flow cytometry analysis showed that Hes6 knockdown induced mildly ineffective erythropoiesis, as reflected by decreased RBCs in spleen and BM (Figure 7H, I). Induced erythroid and megakaryocytic hyperplasia within the BM and spleen has been described in $JAK2^{V617F}$ knock-in mice (28), whereas Hes6 knockdown resulted in a reduction of megakaryocyte hyperplasia in BM and spleen (Figure 7J, K). Additionally, a decrease in thrombus in the lungs was also observed in Hes6 knockdown-recipient mice (Figure 7L). Therefore, *in vivo* results suggest that inhibition of Hes6 is able to ameliorate hyperproliferative phenotypes of PV.

DISCUSSION

Transcription cofactors working in concert with TFs regulate the transcriptional network in cells. In this study, we documented that HES6, the abundantly expressed transcription cofactor in erythroid cells, facilitates erythroid cell proliferation and differentiation during human erythropoiesis. Through immunoprecipitation-related assays, we demonstrated that HES6 is a cofactor of GATA1. Functionally, GATA1 could rescue the development defects in HES6-knockdown erythroblasts, which suggests that HES6 regulates human erythropoiesis through GATA1, and highlights the importance of their interaction in human erythropoiesis.

Further detailed binding domain analysis of GATA1 and HES6 revealed that the N-TAD and C-TAD of GATA1 are required for HES6 binding, and the bHLH and Orange domains of HES6 are required for GATA1 binding. Notably, Kaneko *et al*. reported that the N-TAD and C-TAD are indispensable for the full activity of GATA1 and contribute to erythropoiesis by regulating their overlapping and unique target genes (29). A previous study showed that the bHLH domain of HES6 is critical for transcription activity of the HES6-containing transcription complex; HES6 can directly interact with CREB-binding protein via its basic region within the bHLH domain in HeLa cells (30). Convincingly, we discovered that HES6 promotes the transcription activity and DNA binding occupancy of GATA1, suggesting that the identified interacting domains are critical for optimal GATA1 activity.

Some GATA1-containing transcriptional complex have been revealed in mouse or human erythroid cells. such as the GATA1–FOG1–NuRD complex (31), the GATA1–Scl/TAL1–LMO2–BRG1 complex (32), the GATA1–SWI/SNF complex (33) and the GATA1–

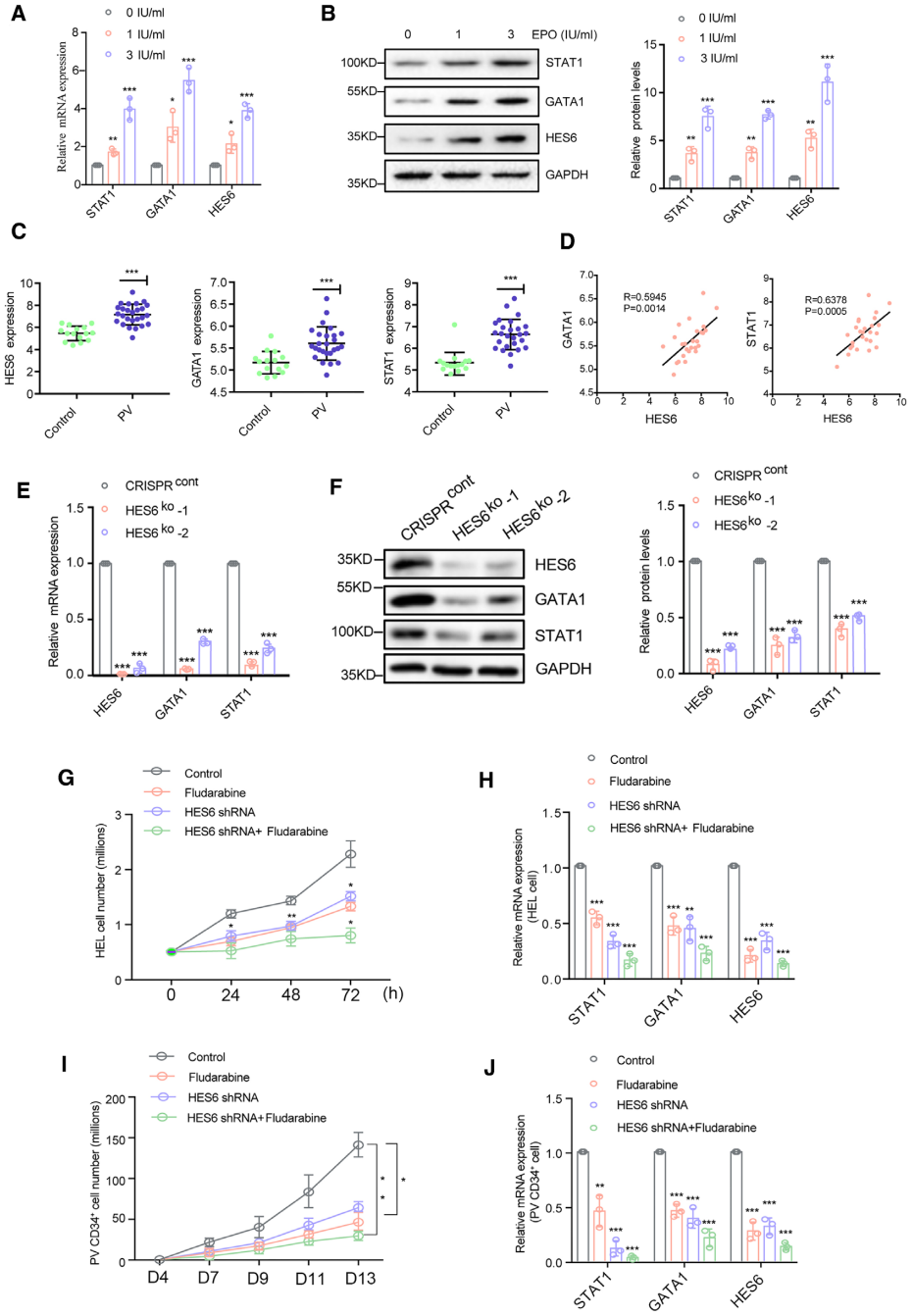

Figure 6. Expression levels and therapeutic implication of the HES6–GATA1 loop in PV patients. (**A**) qRT–PCR results showing HES6, GATA1 and STAT1 mRNA expression levels in cultured primary erythroid cells at day 4 treated with different doses of EPO for 48 h. (**B**) Western blotting analysis of HES6, GATA1 and STAT1 protein expression levels in cultured primary erythroid cells treated with different doses of EPO for 48 h. (**C**) Expression levels of HES6, GATA1 and STAT1 in $CD34^+$ cells from PV patients ($n = 26$), based on the expression profiling by array (GSE103237, $P < 0.0001$). Expression in $CD34^+$ cells from healthy control subjects ($n = 15$) served as the control group. (**D**) Pearson's correlation analysis was performed to analyze the expression correlations between HES6 and GATA1 or STAT1 in $CD34^+$ cells from PV patients at the mRNA expression level. (**E**) qRT–PCR results showing HES6, GATA1 and STAT1 mRNA expression levels in HEL cells infected with lentivirus containing CRISPR-control or two CRISPR-HES6 sgRNAs. (**F**) Representative image of western blotting analysis of HES6, GATA1 and STAT1 expression in HEL cells infected with lentivirus containing CRISPR-control or two CRISPR-HES6 sgRNAs. Right panel: quantitative analysis of protein expression levels from three independent experiments. (**G**) Cell growth curves were determined by manual cell counting of HEL cells infected with control shRNA, HES6 shRNA or treatment with fludarabine (2.5 μM), or HES6 shRNA plus fludarabine (2.5 μM), respectively. (**H**) qRT–PCR analysis of HES6, GATA1 and STAT1 expression in HEL cells infected with control shRNA, HES6 shRNA or treatment with fludarabine (2.5 μM), or HES6 shRNA plus fludarabine (2.5 μM) at 72 h, respectively. (**I**) Cell growth curves were determined by manual cell counting of cultured erythroblasts derived from primary $CD34^+$ cells from PV individuals infected with control shRNA, HES6 shRNA, fludarabine (2.5 μM) and HES6 shRNA plus fludarabine (2.5 μM) ($n = 7$). (**J**) qRT–PCR analysis of HES6, GATA1 and STAT1 expression on day 11 in cultured primary erythroblasts infected with control shRNA, HES6 shRNA, fludarabine (2.5 μM) and HES6 shRNA plus fludarabine (2.5 μM) from PV patients ($n = 7$). Statistical analysis of data from three independent experiments or sample numbers, and the bar plot represents the mean ± SD of triplicate samples. $^*P < 0.05$, $^{**}P < 0.01$, $^{***}P < 0.001$ versus control based on Student's *t*-test.

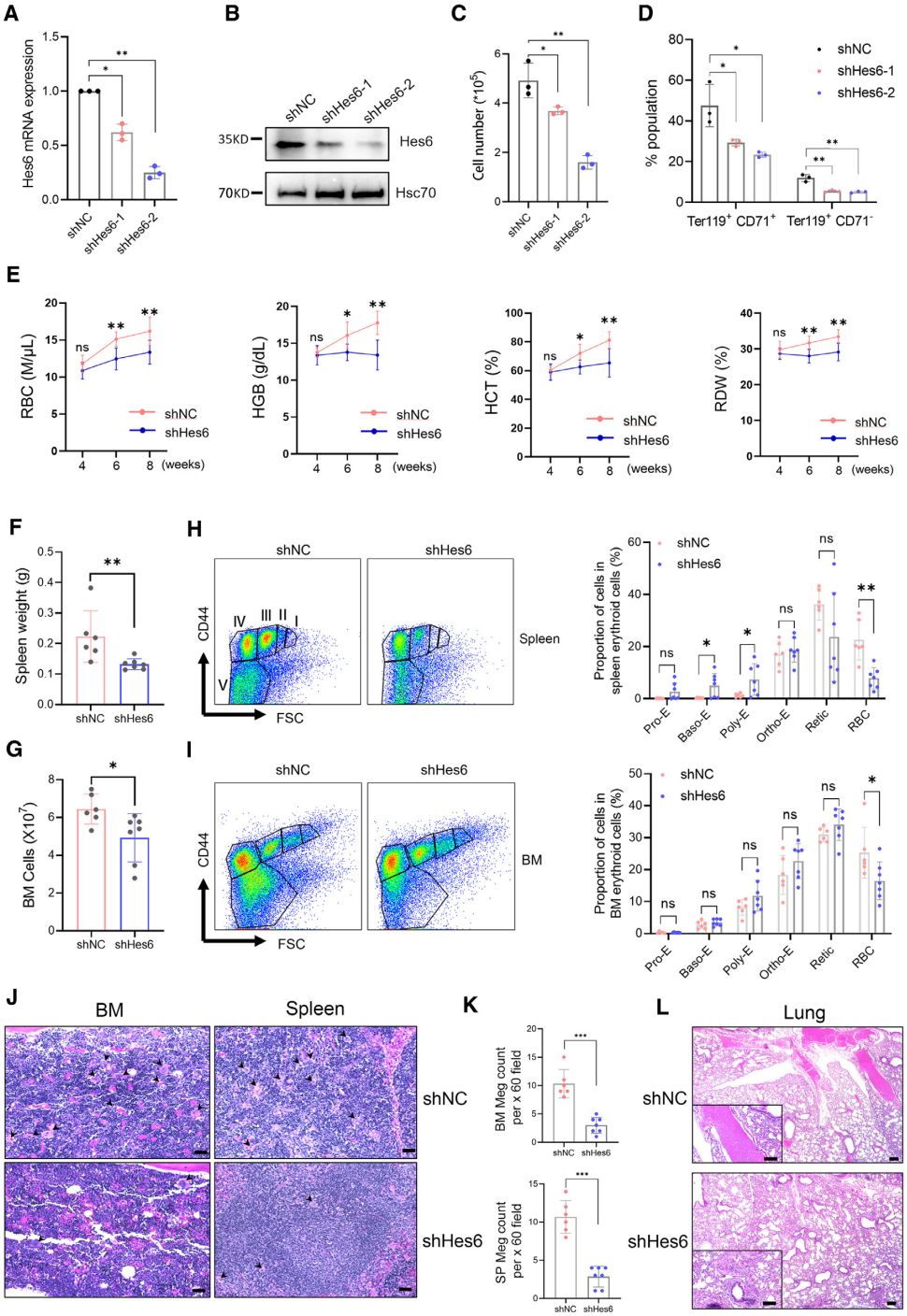

Figure 7. The impact of Hes6 on myeloproliferative phenotypes in JAK2^{V617F} mice. (**A**) qRT–PCR (**A**) and (**B**) western blotting analysis showing Hes6 expression levels in BM lineage-negative cells of C57BL/6 mice infected with lentivirus containing control shRNA or Hes6 shRNA after 48 h of culture. The results were normalized to Hsc70 mRNA and protein levels. (**C**) Quantification of cell number of erythroblasts infected with control shRNA or Hes6 shRNA after 48 h of culture. (**D**) Quantification of erythroblasts infected with control shRNA or Hes6 shRNA at different stages after 48 h of culture by flow cytometry analysis. CD71^{+}TER119^{+} populations are erythroid progenitors, and CD71^{-}TER119^{+} populations are mature erythrocytes. (**E**) Hemocytometer analysis of peripheral blood cells from Hes6 knockdown-recipient mice ($n = 7$) or shRNA control-recipient mice ($n = 6$) at 4, 6 and 8 weeks. (**F**) Quantification of spleen weight of Hes6 knockdown/shRNA control-recipient mice. (**G**) Total bone marrow cell counts from two pelvic bones + two femora + two tibiae of Hes6 knockdown/shRNA control-recipient mice were enumerated by a hemocytometer. (H and I) Erythropoiesis profiles of spleen (**H**) and bone marrow (**I**) of Hes6 knockdown/shRNA control-recipient mice. Representative plots of CD44 versus FSC of the TER119-positive cells with gating of populations I, II, III, IV, V and VI are shown. There is a blockage at the stage from reticulocytes to RBCs. Right panel: the cell distribution analysis based on the flow cytometry results. The bar plot represents the mean ± SD of sample numbers. *P <0.05, **P <0.01 versus control based on Student's t-test. (**J**) H&E staining of bone marrow and spleens of the indicated mice. Arrows indicate megakaryocytes. Scale bars: 100 μm. (**K**) Quantification of megakaryocytes (Meg) in the bone marrow and spleen of the indicated mice. (**L**) H&E staining of lungs of Hes6 knockdown/shRNA control-recipient mice. Inserted are magnifications parts. Scale bars: 100 μm. *P <0.05, **P <0.01 versus control based on Student's t-test.

HDAC5–EKLF–pERK complex (34). Here, through FLAG-HA tandem affinity purification and Co-IP assay, we found that HES6 was present in the GATA1–FOG1–NuRD complex. Specially, HES6 knockdown caused a decrease in the interaction between GATA1 and FOG1. Previous studies show that FOG1 recruits the NuRD complex into association with GATA1 to mediate activation and repression of target genes (35). Thus, the presence of HES6 may be critical for stabilizing the GATA1–FOG1–NuRD complex. Furthermore, through integration of ChIP-seq and RNA-seq, we found that the co-binding regions of HES6 and GATA1 involved several response elements, such as the E-box and ETS-binding elements that have been associated with GATA1 function (23). Interestingly, the GATA1–FOG1 complex could be recruited to a ETS elements by ETS proteins (36). The ETS proteins ERG and SPI1 were also enriched in the co-binding regions of HES6 and GATA1, suggesting that the ETS element may be a key downstream effector for the HES6–GATA1–FOG1 complex. HES6 and GATA1 also co-regulated a series of downstream pathways that have previously been found to be regulated by GATA1 in erythroid cells, such as KIT (37,38), heme (39), RAR (40) and p53 signaling (41). Motif analysis found that the RARα-binding motif is enriched in partial co-binding regions of HES6 and GATA1. GSEA revealed that HES6 is involved in p53-regulated transcription of cell death genes, while HES6 was also reported to be involved in the RAR- (42) and p53 (30)-dependent transcriptional cascades in other cell types. Therefore, HES6 could be a novel transcriptional regulator for these pathways in erythroid cells. Furthermore, we identified a critical positive feedback loop composed of HES6, GATA1 and STAT1 in human erythroid cells. Specifically, we demonstrated that HES6 promoted transcription of the GATA1 gene, while GATA1 reciprocally promoted HES6 gene expression through HES6's upstream TF STAT1. For potential regulatory mechanisms of HES6 on GATA1, through analysis of ChIP-seq data of HES6, we found that no HES6-binding site was observed within 30 kb upstream from the TSS in the GATA1 gene. This suggests that the way in which HES6 regulates GATA1 transcription may not be achieved through binding to the promoter region of GATA1. Whether there is an intermediate TF that mediates the regulatory role of HES6 on the GATA1 gene needs to be further investigated.

For the implication of STAT1 in erythropoiesis, previous studies in mice demonstrated that Stat1-deficient erythroblasts showed delayed differentiation with a reduction in BM-derived CFU-E and increased apoptosis of early erythroblasts (43). Stat1 expression is also significantly down-regulated in Gata1-knockdown murine megakaryocytes. However, the underlying mechanism(s) involved are yet to be fully defined (44); nevertheless, our study supports that there is a positive relationship between GATA1 and STAT1 at transcriptional levels. Furthermore, we found that EPO stimulated expression levels of loop components in erythroblasts. STAT1 is a key effector of EPO–JAK2 signaling through phosphorylation of STAT1 (21,45) and enhancing STAT1 protein expression (46,47). Given that the EPO/JAK2/STAT1 pathway activates genes fundamental for erythroid progenitor development (48,49), we suggest that STAT1 plays a key role in connecting EPO signaling to the HES6–GATA1 loop, contributing to normal erythropoiesis.

Dysregulated JAK2^{V617F}–STAT1 signaling had been implicated in the pathophysiology of PV. Gain-of-function mutation of JAK2^{V617F} contributes to HSC expansion, cell cycling, hyperactivation of growth factors and amplification of the erythroid compartment (24,50,51). To date, little is known about the role of HES6 in PV. Rinaldi *et al*. reported that GATA1 transcription was up-regulated in PV (52). Meyer *et al*. reported activated STAT1 proteins in a JAK2^{V617F} PV patient presenting with extramedullary hematopoiesis in a parailiac mass (53). Shi *et al*. found that JAK2^{V617F}-mediated erythroid terminal hyperproliferation depends on Stat1 overexpression and activation by the constitutively active JAK2^{V617F} kinase in Lin– fetal liver progenitors from mice (47). Our results suggest up-regulation of the loop components involved in erythroid commitment of CD34^{+} cells in PV patients. Importantly, *in vitro*, either knockdown of HES6 or STAT1 inhibition or the enhanced effect by combination of the two in JAK2^{V617F} mutant HEL cells and primary erythroid cells from PV individuals exhibited obvious anti-growth and pro-apoptosis effects. *In vivo*, BM transplantation experiments showed that knockdown of HES6 in BM c-kit+ cells of JAK2^{V617F} mice ameliorates JAK2^{V617F}-induced myeloproliferative phenotypes, as reflected by a decrease in RBC, HGB, HCT, RDW and megakaryocyte hyperplasia in BM and spleen and decreased thrombus in the lungs. These results suggest that restricting HES6–GATA1 regulatory loop levels could be beneficial to control activation of JAK2^{V617F}–STAT1 signaling in JAK2^{V617F}-positive PV.

Collectively, our findings highlight the requirement of the HES6–GATA1 complex and their transcriptional regulatory loop that is regulated by EPO in human erythropoiesis, which provides a novel insight into normal erythropoiesis and a potential therapeutic target for the management of PV.

DATA AVAILABILITY

ChIP-seq and RNA-seq data have been deposited in the National Genomics Data Center (https://ngdc.cncb.ac.cn/?_blank) with the dataset identifier PRJCA011578.

SUPPLEMENTARY DATA

Supplementary Data are available at NAR Online.

ACKNOWLEDGEMENTS

Author contributions: Z.W., J.L. and X.A. designed the experiments. Z.W., P.W., X.H., J.S., N.N., Y.P., Y.L., Y.C., H.L., B.H., L.L., H.L. (Heng Li) and J.Z. performed experiments and analyzed data. Z.W., N.M., P.W. and J.L. drafted the manuscript. J.L., M.Y., H.L. (Hong Liu), K.Y., X.A., N.M., J.M. and H.P. edited the manuscript.

FUNDING

This work was supported by the National Natural Science Foundation of China [81920108004, 81770107,

81702722, 81470362, 81870105, 92253201, 82070175 and U1804282]; the Natural Science Foundation of Hunan Province [2022JJ30787 and 2022JJ30830]; the Science and Technology Key Project of Hunan Province [2018SK21212]; the Scientific Research Fund Project of Hunan Provincial Health Commission [20201921]; Central South University Innovation-Driven Research Programme [2023CXQD015]; Fundamental Research Funds for the Central Universities of Central South University [2021zzts0085 and 2021zzts0562]; Natural Science Foundation of Changsha City [kq2202121]; the National Institute of Health [HL149626 and HL140625] and Postgraduate Scientific Research Innovation Project of Hunan Province [CX20220132].

Conflict of interest statement. None declared.

REFERENCES

1. Hu,J., Liu,J., Xue,F., Halverson,G., Reid,M., Guo,A., Chen,L., Raza,A., Galili,N., Jaffray,J. *et al.* (2013) Isolation and functional characterization of human erythroblasts at distinct stages: implications for understanding of normal and disordered erythropoiesis in vivo. *Blood*, **121**, 3246–3253.
2. Shih,L.Y., Lee,C.T., See,L.C., Ou,Y.C., Dunn,P., Wang,P.N., Kuo,M.C. and Wu,J.H. (1998) In vitro culture growth of erythroid progenitors and serum erythropoietin assay in the differential diagnosis of polycythaemia. *Eur. J. Clin. Invest.*, **28**, 569–576.
3. Wang,Z., Wang,P., Li,Y., Peng,H., Zhu,Y., Mohandas,N. and Liu,J.(2021)Interplay between cofactors and transcription factors in hematopoiesis and hematological malignancies. *Signal Transduct. Target. Ther.*, **6**, 24.
4. Miccio,A., Wang,Y., Hong,W., Gregory,G.D., Wang,H., Yu,X., Choi,J.K., Shelat,S., Tong,W., Poncz,M. *et al.* (2010) NuRD mediates activating and repressive functions of GATA-1 and FOG-1 during blood development. *EMBO J.*, **29**, 442–456.
5. Cantor,A.B. and Orkin,S.H. (2002) Transcriptional regulation of erythropoiesis: an affair involving multiple partners. *Oncogene*, **21**, 3368–3376.
6. Love,P.E., Warzecha,C. and Li,L. (2014) Ldb1 complexes: the new master regulators of erythroid gene transcription. *Trends Genet.*, **30**, 1–9.
7. Bae,S., Bessho,Y., Hojo,M. and Kageyama,R. (2000) The bHLH gene Hes6, an inhibitor of Hes1, promotes neuronal differentiation. *Development*, **127**, 2933–2943.
8. Koyano-Nakagawa,N., Kim,J., Anderson,D. and Kintner,C. (2000) Hes6 acts in a positive feedback loop with the neurogenins to promote neuronal differentiation. *Development*, **127**, 4203–4216.
9. Gao,X., Chandra,T., Gratton,M.O., Quélo,I., Prud'homme,J., Stifani,S. and St-Arnaud,R. (2001) HES6 acts as a transcriptional repressor in myoblasts and can induce the myogenic differentiation program. *J. Cell Biol.*, **154**, 1161–1171.
10. Jhas,S., Ciura,S., Belanger-Jasmin,S., Dong,Z., Llamosas,E., Theriault,F.M., Joachim,K., Tang,Y., Liu,L., Liu,J. *et al.* (2006) Hes6 inhibits astrocyte differentiation and promotes neurogenesis through different mechanisms. *J. Neurosci.*, **26**, 11061–11071.
11. Wang,Y., Li,W., Schulz,V.P., Zhao,H., Qu,X., Qi,Q., Cheng,Y., Guo,X., Zhang,S., Wei,X. *et al.* (2021) Impairment of human terminal erythroid differentiation by histone deacetylase 5 deficiency. *Blood*, **138**, 1615–1627.
12. Basak,A., Munschauer,M., Lareau,C.A., Montbleau,K.E., Ulirsch,J.C., Hartigan,C.R., Schenone,M., Lian,J., Wang,Y., Huang,Y. *et al.* (2020) Control of human hemoglobin switching by LIN28B-mediated regulation of BCL11A translation. *Nat. Genet.*, **52**, 138–145.
13. Quentmeier,H., MacLeod,R.A., Zaborski,M. and Drexler,H.G. (2006) JAK2 V617F tyrosine kinase mutation in cell lines derived from myeloproliferative disorders. *Leukemia*, **20**, 471–476.
14. Goldman,A.R., Beer,L.A., Tang,H.Y., Hembach,P., Zayas-Bazan,D. and Speicher,D.W. (2019) Proteome analysis using gel-LC-MS/MS. *Curr. Protoc. Protein Sci.*, **96**, e93.
15. An,X., Schulz,V.P., Li,J., Wu,K., Liu,J., Xue,F., Hu,J., Mohandas,N. and Gallagher,P.G. (2014) Global transcriptome analyses of human and murine terminal erythroid differentiation. *Blood*, **123**, 3466–3477.
16. Hosoya,T., Clifford,M., Losson,R., Tanabe,O. and Engel,J.D. (2013) TRIM28 is essential for erythroblast differentiation in the mouse. *Blood*, **122**, 3798–3807.
17. Sengupta,T., Cohet,N., Morlé,F. and Bieker,J.J. (2009) Distinct modes of gene regulation by a cell-specific transcriptional activator. *Proc. Natl Acad. Sci. USA*, **106**, 4213–4218.
18. Tallack,M.R., Magor,G.W., Dartigues,B., Sun,L., Huang,S., Fittock,J.M., Fry,S.V., Glazov,E.A., Bailey,T.L. and Perkins,A.C. (2012) Novel roles for KLF1 in erythropoiesis revealed by mRNA-seq. *Genome Res.*, **22**, 2385–2398.
19. Rogers,H., Wang,L., Yu,X., Alnaeeli,M., Cui,K., Zhao,K., Bieker,J.J., Prchal,J., Huang,S., Weksler,B. *et al.* (2012) T-cell acute leukemia 1 (TAL1) regulation of erythropoietin receptor and association with excessive erythrocytosis. *J. Biol. Chem.*, **287**, 36720–36731.
20. Wang,P., Wang,Z. and Liu,J. (2020) Role of HDACs in normal and malignant hematopoiesis. *Mol. Cancer*, **19**, 5.
21. Gallagher,P.G., Liem,R.I., Wong,E., Weiss,M.J. and Bodine,D.M. (2005) GATA-1 and Oct-1 are required for expression of the human alpha-hemoglobin-stabilizing protein gene. *J. Biol. Chem.*, **280**, 39016–39023.
22. Wu,J., Zhou,L.Q., Yu,W., Zhao,Z.G., Xie,X.M., Wang,W.T., Xiong,J., Li,M., Xue,Z., Wang,X. *et al.* (2014) PML4 facilitates erythroid differentiation by enhancing the transcriptional activity of GATA-1. *Blood*, **123**, 261–270.
23. Chlon,T.M., Doré,L.C. and Crispino,J.D. (2012) Cofactor-mediated restriction of GATA-1 chromatin occupancy coordinates lineage-specific gene expression. *Mol. Cell*, **47**, 608–621.
24. Kirito,K., Nakajima,K., Watanabe,T., Uchida,M., Tanaka,M., Ozawa,K. and Komatsu,N. (2002) Identification of the human erythropoietin receptor region required for Stat1 and Stat3 activation. *Blood*, **99**, 102–110.
25. Zhao,W., Kitidis,C., Fleming,M.D., Lodish,H.F. and Ghaffari,S. (2006) Erythropoietin stimulates phosphorylation and activation of GATA-1 via the PI3-kinase/AKT signaling pathway. *Blood*, **107**, 907–915.
26. Jamieson,C.H., Gotlib,J., Durocher,J.A., Chao,M.P., Mariappan,M.R., Lay,M., Jones,C., Zehnder,J.L., Lilleberg,S.L. and Weissman,I.L. (2006) The JAK2 V617F mutation occurs in hematopoietic stem cells in polycythemia vera and predisposes toward erythroid differentiation. *Proc. Natl Acad. Sci. USA*, **103**, 6224–6229.
27. Lee,S.A., Kim,J.Y., Choi,Y., Kim,Y. and Kim,H.O. (2016) Application of mutant JAK2V617F for in vitro generation of red blood cells. *Transfusion (Paris)*, **56**, 837–843.
28. Li,J., Spensberger,D., Ahn,J.S., Anand,S., Beer,P.A., Ghevaert,C., Chen,E., Forrai,A., Scott,L.M., Ferreira,R. *et al.* (2010) JAK2 V617F impairs hematopoietic stem cell function in a conditional knock-in mouse model of JAK2 V617F-positive essential thrombocythemia. *Blood*, **116**, 1528–1538.
29. Kaneko,H., Kobayashi,E., Yamamoto,M. and Shimizu,R. (2012) N- and C-terminal transactivation domains of GATA1 protein coordinate hematopoietic program. *J. Biol. Chem.*, **287**, 21439–21449.
30. Eun,B., Lee,Y., Hong,S., Kim,J., Lee,H.W., Kim,K., Sun,W. and Kim,H. (2008) Hes6 controls cell proliferation via interaction with cAMP-response element-binding protein-binding protein in the promyelocytic leukemia nuclear body. *J. Biol. Chem.*, **283**, 5939–5949.
31. Hong,W., Nakazawa,M., Chen,Y.Y., Kori,R., Vakoc,C.R., Rakowski,C. and Blobel,G.A. (2005) FOG-1 recruits the NuRD repressor complex to mediate transcriptional repression by GATA-1. *EMBO J.*, **24**, 2367–2378.
32. Tripic,T., Deng,W., Cheng,Y., Zhang,Y., Vakoc,C.R., Gregory,G.D., Hardison,R.C. and Blobel,G.A. (2009) SCL and associated proteins distinguish active from repressive GATA transcription factor complexes. *Blood*, **113**, 2191–2201.
33. Xu,Z., Meng,X., Cai,Y., Koury,M.J. and Brandt,S.J. (2006) Recruitment of the SWI/SNF protein Brg1 by a multiprotein complex effects transcriptional repression in murine erythroid progenitors. *Biochem. J.*, **399**, 297–304.
34. Varricchio,L., Dell'Aversana,C., Nebbioso,A., Migliaccio,G., Altucci,L., Mai,A., Grazzini,G., Bieker,J.J. and Migliaccio,A.R. (2014) Identification of NuRSERY, a new functional HDAC complex

composed by HDAC5, GATA1, EKLF and pERK present in human erythroid cells. *Int. J. Biochem. Cell Biol.*, **50**, 112–122.
35. Snow,J.W. and Orkin,S.H. (2009) Translational isoforms of FOG1 regulate GATA1-interacting complexes. *J. Biol. Chem.*, **284**, 29310–29319.
36. Wang,X., Crispino,J.D., Letting,D.L., Nakazawa,M., Poncz,M. and Blobel,G.A. (2002) Control of megakaryocyte-specific gene expression by GATA-1 and FOG-1: role of Ets transcription factors. *EMBO J.*, **21**, 5225–5234.
37. Yang,L., Chen,Z., Stout,E.S., Delerue,F., Ittner,L.M., Wilkins,M.R., Quinlan,K.G.R. and Crossley,M. (2020) Methylation of a CGATA element inhibits binding and regulation by GATA-1. *Nat. Commun.*, **11**, 2560.
38. Jing,H., Vakoc,C.R., Ying,L., Mandat,S., Wang,H., Zheng,X. and Blobel,G.A. (2008) Exchange of GATA factors mediates transitions in looped chromatin organization at a developmentally regulated gene locus. *Mol. Cell*, **29**, 232–242.
39. Doty,R.T., Yan,X., Lausted,C., Munday,A.D., Yang,Z., Yi,D., Jabbari,N., Liu,L., Keel,S.B., Tian,Q. *et al.* (2019) Single-cell analyses demonstrate that a heme–GATA1 feedback loop regulates red cell differentiation. *Blood*, **133**, 457–469.
40. Dewamitta,S.R., Joseph,C., Purton,L.E. and Walkley,C.R. (2014) Erythroid-extrinsic regulation of normal erythropoiesis by retinoic acid receptors. *Br. J. Haematol.*, **164**, 280–285.
41. Trainor,C.D., Mas,C., Archambault,P., Di Lello,P. and Omichinski,J.G. (2009) GATA-1 associates with and inhibits p53. *Blood*, **114**, 165–173.
42. Kim,S.C., Kim,C.K., Axe,D., Cook,A., Lee,M., Li,T., Smallwood,N., Chiang,J.Y., Hardwick,J.P., Moore,D.D. *et al.* (2014) All-trans-retinoic acid ameliorates hepatic steatosis in mice by a novel transcriptional cascade. *Hepatology*, **59**, 1750–1760.
43. Halupa,A., Bailey,M.L., Huang,K., Iscove,N.N., Levy,D.E. and Barber,D.L. (2005) A novel role for STAT1 in regulating murine erythropoiesis: deletion of STAT1 results in overall reduction of erythroid progenitors and alters their distribution. *Blood*, **105**, 552–561.
44. Muntean,A.G. and Crispino,J.D. (2005) Differential requirements for the activation domain and FOG-interaction surface of GATA-1 in megakaryocyte gene expression and development. *Blood*, **106**, 1223–1231.
45. Voisset,E., Lopez,S., Dubreuil,P. and De Sepulveda,P. (2007) The tyrosine kinase FES is an essential effector of KITD816V proliferation signal. *Blood*, **110**, 2593–2599.
46. Chai,H.T., Yip,H.K., Sun,C.K., Hsu,S.Y. and Leu,S. (2016) AG490 suppresses EPO-mediated activation of JAK2–STAT but enhances blood flow recovery in rats with critical limb ischemia. *J. Inflamm. (Lond.)*, **13**, 18.
47. Shi,J., Yuan,B., Hu,W. and Lodish,H. (2016) JAK2 V617F stimulates proliferation of erythropoietin-dependent erythroid progenitors and delays their differentiation by activating Stat1 and other nonerythroid signaling pathways. *Exp. Hematol.*, **44**, 1044–1058.
48. Sangrar,W., Gao,Y., Bates,B., Zirngibl,R. and Greer,P.A. (2004) Activated Fps/Fes tyrosine kinase regulates erythroid differentiation and survival. *Exp. Hematol.*, **32**, 935–945.
49. Cokic,V.P., Bhattacharya,B., Beleslin-Cokic,B.B., Noguchi,C.T., Puri,R.K. and Schechter,A.N. (2012) JAK–STAT and AKT pathway-coupled genes in erythroid progenitor cells through ontogeny. *J. Transl. Med.*, **10**, 116.
50. Lundberg,P., Takizawa,H., Kubovcakova,L., Guo,G., Hao-Shen,H., Dirnhofer,S., Orkin,S.H., Manz,M.G. and Skoda,R.C. (2014) Myeloproliferative neoplasms can be initiated from a single hematopoietic stem cell expressing JAK2-V617F. *J. Exp. Med.*, **211**, 2213–2230.
51. Geron,I., Abrahamsson,A.E., Barroga,C.F., Kavalerchik,E., Gotlib,J., Hood,J.D., Durocher,J., Mak,C.C., Noronha,G., Soll,R.M. *et al.* (2008) Selective inhibition of JAK2-driven erythroid differentiation of polycythemia vera progenitors. *Cancer Cell*, **13**, 321–330.
52. Rinaldi,C.R., Martinelli,V., Rinaldi,P., Ciancia,R. and del Vecchio,L. (2008) GATA1 is overexpressed in patients with essential thrombocythemia and polycythemia vera but not in patients with primary myelofibrosis or chronic myelogenous leukemia. *Leuk. Lymphoma*, **49**, 1416–1419.
53. Meyer,T., Ruppert,V., Görg,C. and Neubauer,A. (2010) Activated STAT1 and STAT5 transcription factors in extramedullary hematopoietic tissue in a polycythemia vera patient carrying the JAK2 V617F mutation. *Int. J. Hematol.*, **91**, 117–120.